61

非一様気体中を伝播する衝撃波の数値解析

藤本仁*1, 石井隆次*1, 八田夏夫*1, 梅田吉邦*2

Numerical Analysis of Shock Waves in Nonuniform Gas

by

Hitoshi Fujimoto*1, Ryuji Ishii*1, Natsuo Hatta*1, and Yoshikuni Umeda*2

ABSTRACT

Instability of shock waves propagating through a stratified gas is investigated numerically. A shock wave is produced by a piston which begins to move from rest abruptly at some constant velocity in a two-dimensional horizontal duct. Initially the gas in the duct has a temperature or density distribution only along the vertical axis at a constant pressure. The initial density distribution, which is assumed to change monotonically, has zero spatial gradient at the upper and lower walls and then has a single inflection point. Numerical simulations are performed for the weak density nonuniformity, where a substantially steady curved shock can be realized at least for some time interval in the shock evolution. It is shown that the curved shock front tends to be disturbed by pressure fluctuations which are produced by nonlinear interactions between the instability waves and the shock-induced flow field. At a high Reynolds number the gas viscosity does not affect appreciably the instability waves. The gas viscosity, however, plays an important role in stabilizing the shock front against the pressure fluctuations.

I. INTRODUCTION

Shock propagation in nonuniform gas is realized in many practical situations. Here shock waves propagating through a stratified gas were investigated numerically in detail using a TVD-scheme with the Euler and the Navier-Stokes equations. We consider the same system as that treated in the previous paper (1). The system is composed of an ideal gas in a two-dimensional horizontal duct at some constant pressure. Initially, the gas in the duct is at rest and has a density or temperature distribution only along the vertical direction. The density distribution which changes monotonically in the vertical direction, has zero spatial gradient at the lower and upper walls, and has a single inflection point. At time t = 0, a piston in the duct begins to move from rest at some constant velocity to produce a shock in front of it.

In the previous paper (1), an analytical solution for the substantially steady curved shock was obtained in the coordinate system fixed on the shock. It was shown that the analytical results in the linearized problem for the Euler equations predict the numerical results well for the weak density inhomogeneity. The flow instability of this shock-induced flow was also investigated. The pressure fluctuations observed in the numerical results are consistent with the theoretical predictions for the Euler equations. Although the instability waves do not affect the shock front in the context of the linear analysis, the actual induced flow field is nonlinear and then the development of the instability waves may eventually affect the shock front at a very large time. This nonlinear problem has not yet been resolved.

In light of this, we will investigate in detail the shock behavior and the time evolution of the shock induced flow. It will be shown that pressure waves produced by nonlinear interactions between the instability waves and the shock-induced flow field tend to disturb the shock front. But, the gas viscosity plays an important role in suppressing the pressure fluctuations and also in stabilzing the shock front.

II. NUMERICAL SIMULATION

Consider a two-dimensional duct with a constant cross

*1 京都大学大学院エネルギー科学研究科

*2 京都大学大学院工学研究科

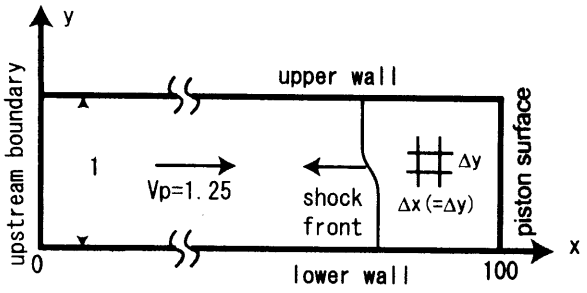

Fig.1 Schematic flow system

section as shown in Fig.1, where x is the horizontal axis and y is the vertical one and a piston is placed at the right end. Initially the gas pressure p_∞ is constant and the gas density ρ_∞ is given as a function of y, $\rho_\infty=\rho_\infty(y)$, which means that the gas temperature T_∞ is given as a function of y, $T_\infty=T_\infty(y)$, through the equation of state, where the subscript ∞ represents the initial gas conditions. At time t=0, the piston begins to move from rest at a constant velocity V_p into the left ($-x$) direction. For analytical convenience, however, we consider an equivalent system where the gas has initially a uniform velocity V_p and begins to impinge at t=0 on the piston surface fixed at the right end. It is noted that physical properties are represented in dimensionless form based on the initial conditions and the duct width. We consider two types of density profile,

$$\rho_\infty = \bar{\rho}_\infty[1+\varepsilon f(y)], \tag{1}$$

where

$$f(y) = \cos(\pi y) \tag{2}$$

and

$$f(y) = \begin{cases} -1 & \text{for } \frac{1}{2}+\delta \le y \le 1 \\ -\frac{1}{\delta}\left(y-\frac{1}{2}\right) & \text{for } \frac{1}{2}-\delta \le y \le \frac{1}{2}+\delta \\ 1 & \text{for } 0 \le y \le \frac{1}{2}-\delta \end{cases} \tag{3}$$

where $\bar{\rho}_\infty$ is an averaged value of the gas density ρ_∞ over the duct cross section. The parameters ε and δ are chosen as ε=0.2 for the cosine density distribution, ε=0.1, δ=0.1 for the piece-wise linear density distribution.

III. NUMERICAL RESULTS

A. Numerical Accuracy

In the numerical simulations, the piston velocity is chosen as V_p=1.25 which means that the gas impinges on the fixed piston surface at a velocity u_∞=1.25 through the coordinate transformation as in Ref. 1. On the piston surface and the duct walls, the symmetric conditions are applied for the Euler equations and the no-slip conditions are applied for the Navier-Stokes equations. The time interval is chosen to be $\Delta t=C_{FL}\times\min(\Delta x, \Delta y)/[C+(u^2+v^2)^{1/2}]$, where C_{FL}=0.2 and Δx and Δy are the spatial mesh sizes. Square meshes are employed and their sizes are set to $\Delta x=\Delta y$=0.02 and 0.01. In what follows, the former is called the coarse mesh and the latter the fine mesh. The computational domain is 100×1 where the upstream boundary is located at x=0 and the piston surface is at x=100. The integration time interval is $0 \le t \le 120$. The ratio of specific heats of the gas, γ, is chosen to be 1.4 and the Prandtl number, Pr, to be 0.76. The numerical simulations were performed for both the coarse and fine meshes in each case.

In the Navier-Stokes calculation, the duct height H is taken to be 2.0 cm, which yields the Reynolds number of 4.6×10^5 based on the sound velocity at S.T.P. Another Reynolds number of 4.6×10^3 is also applied to investigate viscous effects on the numerical results. In such cases, development of the shock-induced boundary layer will be neglected. Although it is impossible to predict the inner structure of shock front numerically even with the Navier-Stokes equations, it will be possible to evaluate

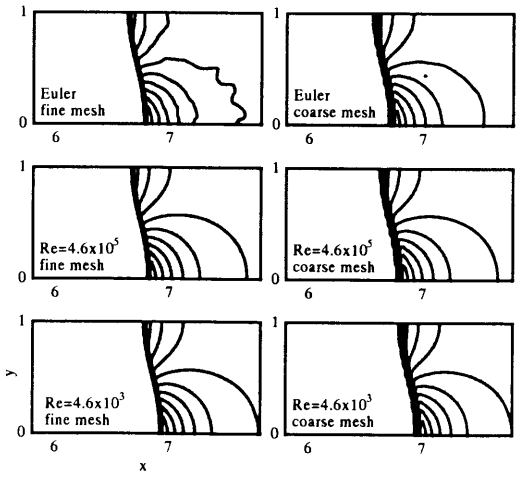

Fig. 2 Shock profiles at t=120 for the cosine density distribution.

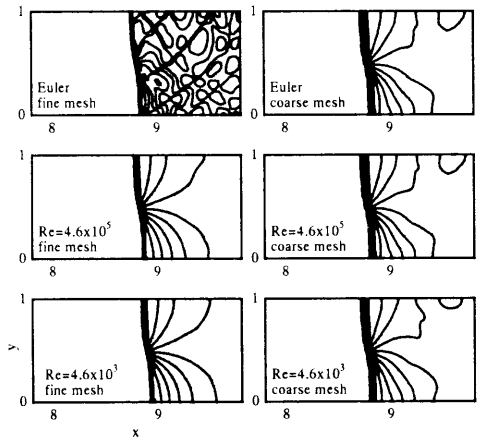

Fig. 3 Shock profiles at t=120 for the piece-wise linear density distribution.

the viscous effect on the shock induced flow in the core region between the upper and lower boundary layers. The thermal boundary conditions at the upper and the lower walls are set to $\partial T/\partial y = 0$. As described above, we cannot capture the boundary layers numerically, but the result will be creditable under the assumption that the boundary layers are negligibly thin. The results are compared with the corresponding inviscid ones.

The present TVD-scheme can predict the Rankine-Hugoniot relations within the accuracy of 99.8 % for the one dimensional shock tube problem. The numerical accuracy of the two-dimensional results depends on the mesh size (2). In Figs. 2 and 3, the shock profiles at t= 120 are shown for the cosine and the piece-wise linear density distributions, respectively. Agreement among all

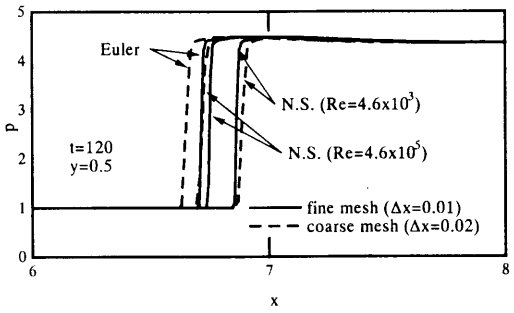

Fig. 4 Shock fronts at t=120 for the cosine density distribution.

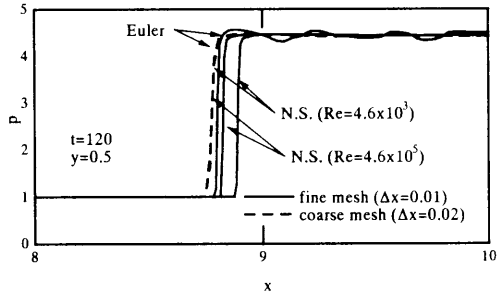

Fig. 5 Shock fronts at t=120 for the piece-wise linear density distribution.

shock profiles (except for their locations) is remarkable for each type of density distribution. The pressure contours show some differences among them especially for the piece-wise linear density distribution. Considering the numerical accuracy, however, it will be reasonable to say that even the shock-induced flow fields near the fronts show fairly good agreement among them. Only the pressure contours in the inviscid results with the fine mesh show appreciable fluctuations, which will be produced by pressure disturbances propagating upstream from the downstream flow region. We can conclude that satisfactory mesh-convergency was obtained numerically both for the inviscid and viscous results except for the pressure fluctuations in the shock induced flow fields. Since the instability in the downstream region of the shock front is responsible for generation of these pressure fluctuations, the details about them are discussed below again in relation to the instability waves.

For more closer investigation of .the numerical accuracy, pressure profiles along the centerline y = 1/2 near the shock front are shown in Figs. 4 and 5. Considering the fact that the distance between the shock front and the piston surface is about 93 at t = 120, the difference among them is very slight. For example, the distance between the shock fronts for the Euler equations with the fine and coarse meshes in Fig. 4 is about 0.05 which is 0.06 percent of the distance between the shock front and the piston surface. Since the numerical accuracies in time and space are the second

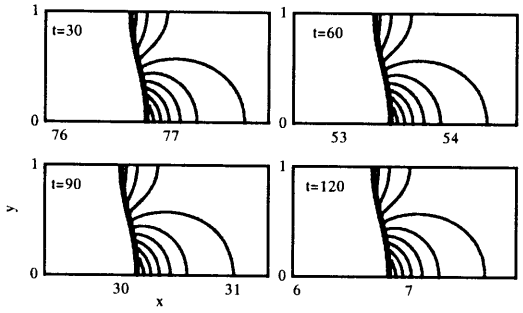

Fig. 6 Time evolution of shock profiles for the cosine density distribution; Re=4.6×10^5.

order, it will be reasonable to consider that the mesh convergency for the shock profile in each case is well realized. The locations of shock front for the coarse mesh do not depend on the Reynolds number for the piece-wise linear density distribution. Numerically locations of all the fronts coincide completely in Fig. 5. Although the shock speed seems to depend slightly on the Reynolds number, that is, the shock front for a higher Reynolds number seems to be faster than that for a lower Reynolds number, the difference between them at t = 120 may be within the possible numerical error.

B. Time-change of Shock Profile

Next, consider the time change of the shock profile and the induced flow field near the shock front. In Figs. 6 and 7, the shock profiles are shown at t = 30, 60, 90 and 120. In the viscous results, time-convergency of the

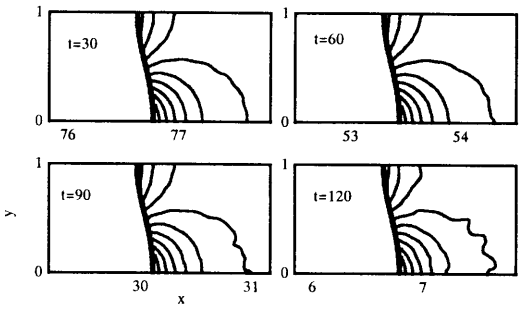

Fig. 7 Time evolution of shock profiles for the cosine density distribution; Re=∞.

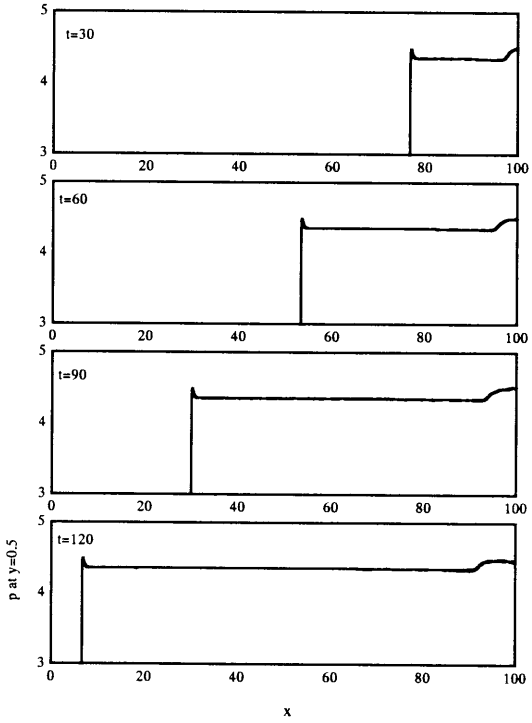

Fig. 8 Pressure profiles along the centerline (y=1/2) for the cosine density distribution calculated using the coarse mesh; Re=∞.

shock profile is quite remarkable. Numerically it was confirmed that the shock profile remains unchanged for t > 3. In the inviscid results of Fig. 7, the situation is a little different. For 3 < t < 120, the shock profile itself is substantially unchanged, but the induced flow field near the shock front begins to be disturbed for t > 30.

C. Instability Waves

In order to investigate the instability waves and pressure fluctuations produced by nonlinear interactions between the instability waves and the shock-induced flow field, time-change of pressure profiles along y = 1/2 is shown in Figs. 8 to 11. Figures 8 and 9 show inviscid results for the cosine density distribution which correspond to Fig. 2. In the results with coarse mesh in Fig. 8, only slight pressure fluctuations are seen. However, the results with the fine mesh in Fig. 9 have serious fluctuations which are enhanced with increasing time. These fluctuations are obviously mesh dependent and then will not show physical phenomena. These are

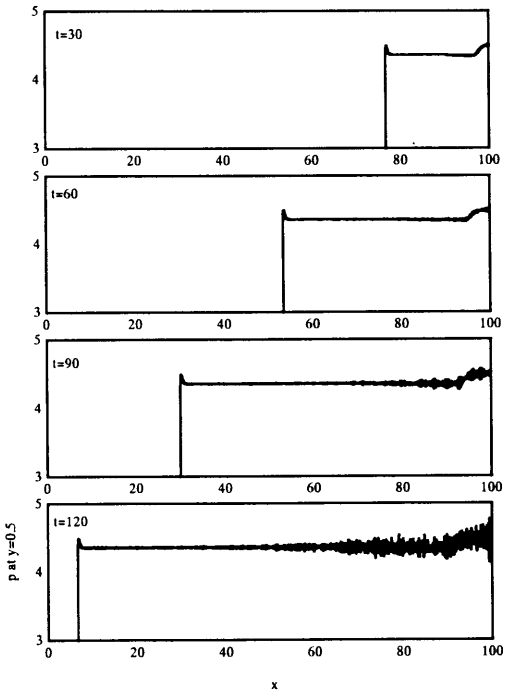

Fig. 9 Pressure profiles along the centerline (y=1/2) for the cosine density distribution calculated using the fine mesh; Re=∞.

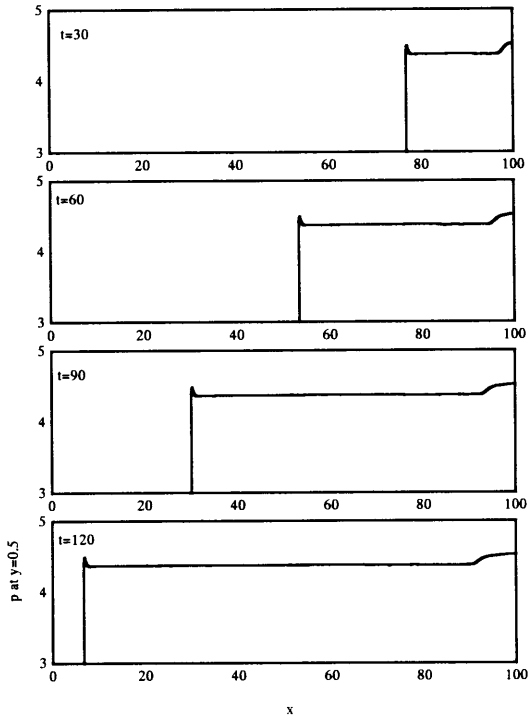

Fig. 10 Pressure profiles along the centerline (y=1/2) for the cosine density distribution calculated using the coarse mesh; Re=4.6×10^5.

perhaps artificial or superficial phenomena inherent to the numerical simulations with the Euler code.

The corresponding viscous results are shown in Figs. 10 and 11 for Re = 4.6×10^5. Any appreciable differences between the results at t = 30, 60, 90 and 120 are not observed in these figures.

Although the instability is relatively very weak for the cosine density distribution and very difficult to observe the instability waves, they are clearly confirmed in the results for the piece-wise linear density distribution as shown in Figs. 12. Numerically it was confirmed that main frequency characteristics do not depend on the mesh size for Re=4.6×10^5 and for Re=4.6×10^3. This suggests that numerical results will have physical meanings. The generation, growing and propagation of the instability waves do not depend appreciably on the Reynolds numbers, at least, greater than 4.6×10^3. It is also well demonstrated that higher modes of instability waves grow with increasing time.

It has to be stressed that these pressure waves are composed of the original instability waves produced by the flow instability and the pressure waves produced by the nonlinear interactions between the instability waves and the flow fields. Since the instability waves may have various wavelengths, we can not distinguish completely the induced pressure waves from the instability waves.

IV. CONCLUSIONS

Instability of shock waves propagating through a stratified gas was investigated numerically. Our previous analysis has predicted that substantially steady curved shocks in the coordinate system fixed on the shock are stable in the context of the linear analysis. But the present numerical simulations showed that pressure waves are produced owing to interactions between the instability waves and the shock induced flow field. They can propagate upstream as well as downstream and can reach the shock front and tend to disturb it with increasing time. The gas viscosity is effective to suppress the pressure fluctuations. At a high Reynolds number,

however, the gas viscosity affects slightly growing and propagation of the instability waves.

References

1) R. Ishii, H. Fujimoto, N. Hatta, Y. Umeda and M. Yuhi, "Shock waves in nonuniform gas", PHYSICS OF FLUIDS, Vol.11, (1999), pp.1921-1935.

2) R. Ishii, H. Fujimoto, N. Hatta and Y. Umeda, "Experimental and numerical analysis of circular pulse jets", Journal of Fluid Mech., vol.392, (1999), pp. 129-154..

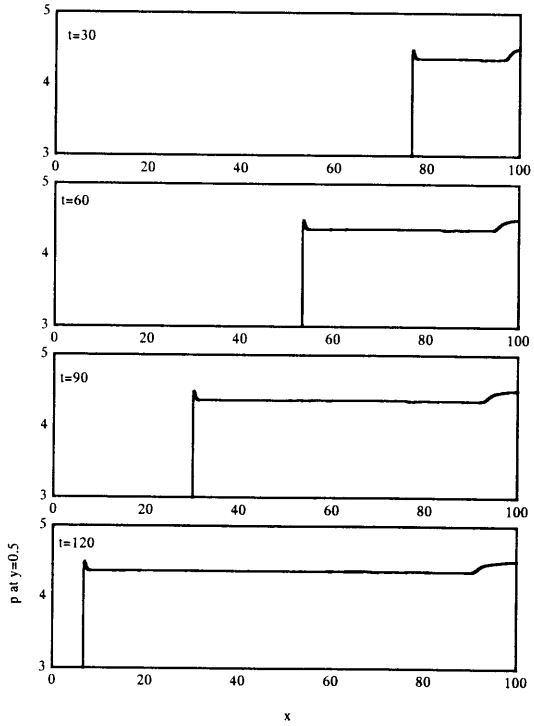

Fig. 11 Pressure profile along the centerline (y=1/2) for the cosine density distribution with the fine mesh; Re=4.6×10^5.

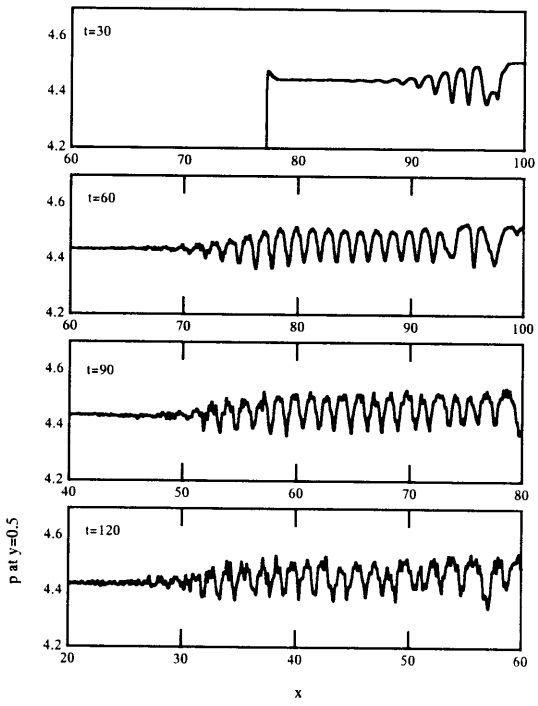

Fig. 12 Pressure profile along the centerline (y=1/2) for the piece-wise linear density distribution with the fine mesh; Re=4.6×10^5.